ESOMAT 2009, 05009 (2009)
DOI:10.1051/esomat/200905009

Microstructural investigations of laser welded dissimilar Nickel-Titanium-steel joints

H. Gugel[a] and W. Theisen

Ruhr-Universität Bochum, Institut für Werkstoffe, Universitätsstr. 150, 44801 Bochum, Germany

Abstract. Nickel-titanium based shape memory alloys are used in a variety of applications. These applications desire joining techniques that provide only local degradation of the functional properties and are compatible to the special mechanical properties of shape memory materials. Laser welding of nickel-titanium based shape memory alloys is an established process in medical application. Similar and especially dissimilar joints of nickel-titanium shape memory alloys, in particular joints of nickel-titanium and steel, are requested combinations to open additional fields of applications. A detailed investigation of the microstructural changes of laser welded parts is necessary to provide a good weld quality and to consider the related changes of the mechanical properties in the design process for certain applications.
The formation of phases in the heat-affected zone as well as in the fusion zone was investigated by means of optical microscopy, scanning electron microscopy, electron backscatter diffraction and X-Ray diffraction. Focused ion beam was used for aim preparation of transmission electron microscopy samples at the interface nickel-titanium/fusion zone, the center of the fusion zone and the interface fusion zone/steels.

1. Introduction

The application of Nickel-Titanium shape memory alloys (NiTi-SMA) is related to appropriate joining technique. In practical application currently a variety of joining techniques like clamping, crimping, etc. soldering and welding are used for similar joints of NiTi as well as for dissimilar joints of NiTi-SMA to other materials. Especially the joint of NiTi-SMA and iron-based alloys is of special interest for the application. Each of these joining techniques has local influences on the shape memory properties of the NiTi-SMA due to mechanical or the thermal effects of the joining processes. Compared to conventional joining techniques, laser welding affects the shape memory properties only in a very narrow range. Laser welding of similar joints of nickel-titanium shape memory alloys is an established process and was investigated in a variety of studies dealing with CO_2- and Nd:YAG lasers [1], [2]. The investigations focus on the changes of the thermal and mechanical properties of the SMA due to laser welding [3], [4] and [5]. A major problem of joining NiTi to an iron-based alloy by a fusion welding process is the formation of brittle intermetallic phases of the type FeTi, Fe_2Ti and the formation of oxides. Previous work of Hall et al. and Wang et al. described the appearance of cracks directly after welding [6], [7]. Both authors present joints of NiTi and steel with cracks situated on the NiTi-side of the joint. In a previous study on laser welding of NiTi and Steel microwire we showed crack free welds which benefit of the pseudoelastic effect in tensile testing [8], [9]. Because laser welding is an established technique to provide similar joints of NiTi and as well one of the promising processes for joining NiTi-SMA to a dissimilar component, the microstructure of a dissimilar NiTi/AISI 304 joint should be investigated. In the present work the microstructure of the laser welded joint should be characterized with respect to the formation of the different phases of the dissimilar joints.

2. Materials and Experiments

2.1. Material

In this study sheet material of 1mm thickness was used for the production of dissimilar Ni-Ti / steel joints. A pseudoelastic Nickel-Titanium shape memory alloy with a chemical composition of 49.2 at.% Ti, 50.8 at.% Ni and for the steel component an austenitic steel AISI 304 were chosen. The sheet materials were cut into sections of 20 mm x 25 mm. Prior to welding the surface was ground with 500er SiC and cleaned in ethanol.

[a] e-mail: gugel@wtech.rub.de

Article available at http://www.esomat.org or http://dx.doi.org/10.1051/esomat/200905009

2.2. Welding

The laser welding was performed in a square butt joint using a Nd:YAG solid state laser (Trumpf Laser HL 304P). The chosen parameters for the welding process are listed in **Table. 1**. Based on former investigations [8], [9] the laser spot was shifted to the side of NiTi-component by Δx = 70% of the weld pool width (**Fig.1**) in order to adjust a certain microstructure which had led good mechanical properties of joint wires. An argon

Table 1: Laser parameter

Pulse power	1100 W
Pulse width	4 ms
Frequency	50 Hz
Velocity	600 mm/min
Optics	D70, f = 200mm
defocused	0,65 mm

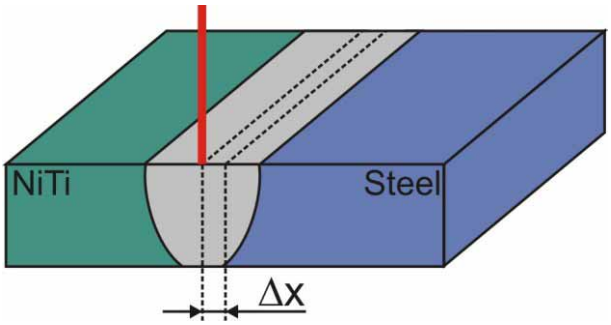

Fig. 1: Schematic illustration of the laser welding process. The right-most broken line marks the joint of the two sheets and Δx is related to the shift of the laser spot from the joint.

shielding at the top and the bottom of the weld pool was used to reduce the formation of oxides. The welding was performed without using filler material. No post-weld heat treatment has been applied.

2.3. Scanning electron microscopy and electron backscatter diffraction

Details of the microstructure were obtained by scanning electron microscopy (SEM) using a LEO 1580VP. For the SEM investigations the samples were subsequently ground and polished down to 0.05 µm. Micrographs were obtained using a BSE-detector. In order to identify the different phases in the fusion zone, electron backscatter diffraction (EBSD) measurements were carried out. The sample was scanned with a take off angle of 70° and an acceleration voltage of U=30 kV. For the overview scan a step size of 4 µm was chosen. The detail at the steel interface was measured with a step size of 0.35µm. The EBSD offline scan was realized including the phases NiTi, Fe_2Ti, $NiTi_2$, Ni_3Ti and γ-Fe. Possibly present oxides were not investigated in this EBSD study.

2.4. X-Ray diffraction

X-Ray diffraction spectra were recorded on a Philips X'pert diffractometer with CuKα radiation (λ=0.1542 nm). A mono-capillary of ∅100 µm was used in order to collect local diffraction data in the different regions of the joint. The samples was mechanically polished down to 0.05 µm and stepwise scanned across the fusion zone from 2θ = 20° to 100°

2.5. Transmissions electron microscopy and focused ion beam

Thin foils with a size of 15x10 µm were prepared by focus ion beam from different parts of the samples. They were taken from the interface of the fusion zone, from the base materials as well as from the center of the fusion zone. The foils were examined by means of a transmission electron microscope Tecnai F20 G² at an acceleration voltage of 200kV. The local chemical composition was analyzed by an attached EDX-unit.

3. Results and discussion

3.1. Microstructure

Fig. 2 shows an overview of the cross-section of the laser welded NiTi-AISI 304 joint. The welding zone can be subdivided into four sections. The base materials, the heat-affected zone on the NiTi-side and the fusion zone. A heat-affected zone on the steel side is not detectable. The chosen laser parameters provide a full penetration of the sheet material. The fusion zone has a sandglass shaped structure. Due to the welding process, necking of the weld has occurred with a width of the weld at the top of about 1000 µm and 900 µm at the bottom. The weld is completely free of major defects like cracks and pores. Details of the microstructures at the interfaces NiTi/fusion zone, the fusion zone and the interface AISI 304/fusions are presented in Fig. 3. The interface of NiTi and the fusion zone is shown in Fig. 3a). A fine white shining zone separates the heat-affected zone from the fusion zone. At this interface an epitaxial growth of the grains is observed. Two types of precipitations are

visible. Roundly shaped (black arrows) and finely branched (here marked by white arrows much better visible in TEM micrographs in Fig. 9b) dark particles containing mainly Titanium and Carbon. In the center of the fusion zone a fine white shining network encloses matrix cells. This highly segregated dendritic structure has solidified from the melt and is prevalent throughout the complete fusion zone. EDX measurements are mainly pointing to a segregation of Ni, Cr and Fe which are enriched in the inter-dendritic regions due to the primary solidification of NiTi-cells and a successive reduction of Ti by TiC-carbide precipitation. This leads to a remarkable decoration of the inter-dendritic regions by the black colored TiC carbide (Fig. 3b).

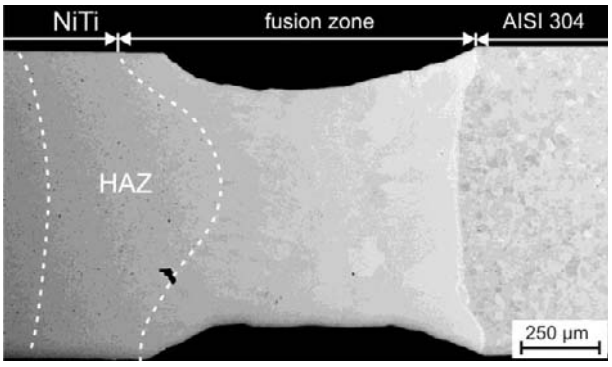

Fig. 2: Overview of the laser welded NiTi/AISI 304 joint. The heat-affected zone (HAZ) is marked by the broken lines.

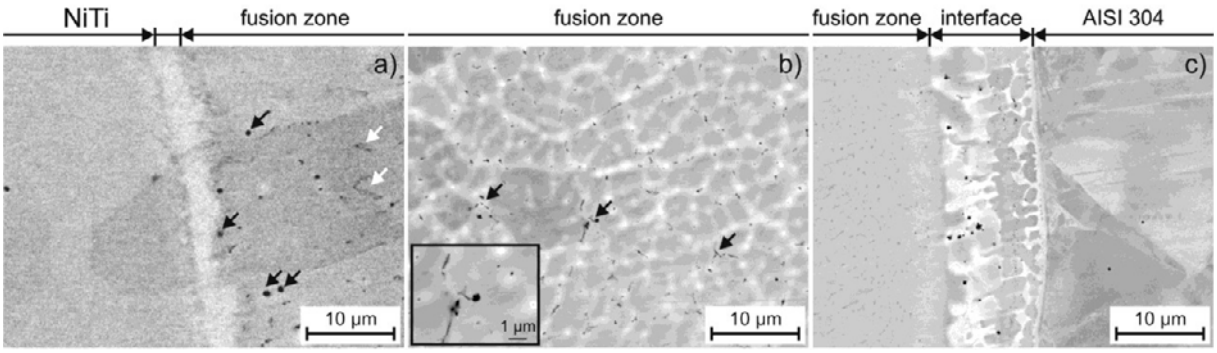

Fig. 3: SEM Micrographs in backscatter electron contrast showing the detail of the joint NiTi-AISI 304 at a) the interface NiTi/fusion zone, b) the fusion zone as well as a detail of the particle in the center and c) at the interface fusion zone/AISI 304.

The interface fusion zone/AISI 304 shows a characteristic coast-line shaped fusion line that separates the fusion zone and the AISI 304. The particle size in the adjacent fusion zone is much smaller compared to the particles in the center of fusion zone (Fig 3c).

3.2. X-Ray diffraction

The local positions of the XRD-measurements are marked by a circle in the optical micrograph of the joint in (Fig. 4). The complete XRD spectra are plotted next to the micrograph. On the NiTi-side and even in the fusion zone the fundamental reflexes (110) (211) and (200) of the B2 structure are present. It should be noticed that the reflex at about 42,5 ° is brought about by the (110)-planes of the B2-Structure and the (111) of the γ-Fe which are overlapping. By moving the measuring positions towards the austenitic steel the two reflexes of the B2 structure (200) and (220) vanish and only the (111) of the austenitic steel is still present. No other reflexes could be detected. Fig. 5 shows the change of the peak at about 42.5° in a higher resolution at different positions in the welding zone. For a better visibility the different positions are plotted with an offset of 50 a.u. in different colors. Starting from the NiTi side (x-position = -600 µm) the intensity decreases while moving the measuring position towards the austenitic steel. At the same time there is a significant drift of the peak to a higher angle. This is due to the fact that the (110) reflex of B2 is vanishing. Finally in the austenitic steel at x = 800 the angle 2θ reaches a value of 42.4°. With a lattice parameter of a = 0.362 which has been reported for AISI 304 [10] 2θ should show a value of 42.9° which is not exactly consistent with the measured angle.

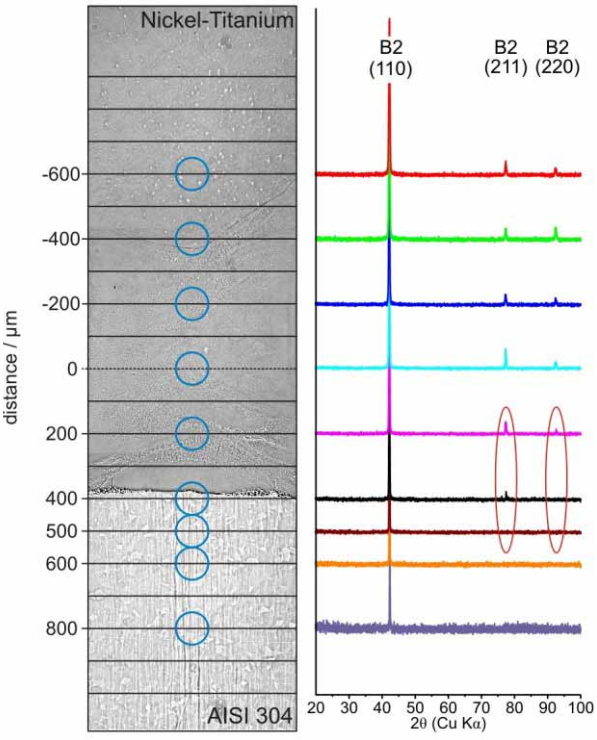

Fig. 4: Optical micrograph of the NiTi-AISI 304 joint cross-section. The circles are marking the measuring positions.

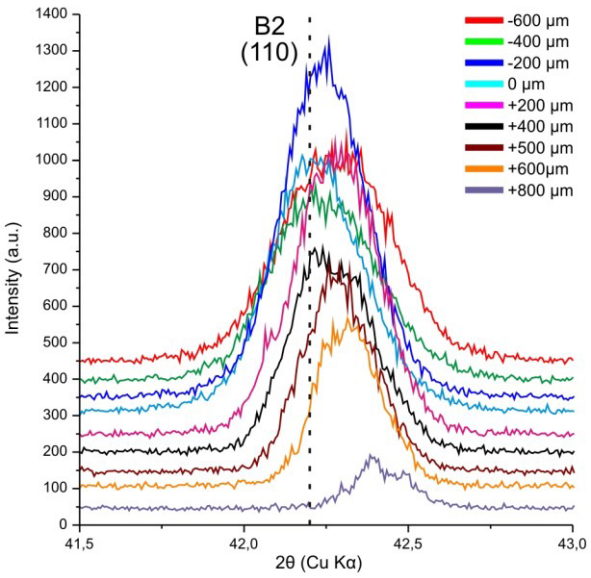

Fig. 5: Shift of the B2 corresponding to the position in the welding zone. The theoretical angle of $2\theta_{B2(110)}$=42.2° for the B2 (110) peak in marked.

3.3. Electron backscatter diffraction (EBSD)

The overview of the grain size distribution in a dissimilar weld joint is shown in Fig 6. On the NiTi-side small equiaxed grains with a size of 20 µm are present in the heat-affected zone in contrast to the larger grain size of 30 µm in the unaffected material. At the interface a massive grain growth in the direction of the thermal gradient is observed. The center of the fusion zone consists of only a few large grains. Close to the interface fusion zone/AISI 304 a directional growth of the grains is present. Based on the shift of the laser spot towards the NiTi-component the grain structure of the AISI 304 base material is sparse influenced.

A map of the different phases is shown in Fig. 7. The overview of the weld reveals that the fusion zone consists of a B2 crystal structure as it has been shown by XRD before. It was not possible to differ between NiTi, FeTi and (Ni, Fe)Ti which a present in the ternary Ni-Ti-Fe-system showing B2 structure with very similar lattice parameter [11, 12]. At the interface fusion zone/AISI 304 additional phases could be detected. A detailed scan of the interface on the steel-side is shown in Fig. 8. The fusion zone has a B2 structure and the AISI 304 has the A1 structure of the γ-Fe. The interface mainly consists of two different phases. The main part of the interface reveals a crystal structure related to the Fe_2Ti Type (blue colored). The small green areas are off a bcc structure t which could be due to the primary solidification δ-Fe as it has been described by Bhadeshia et al. [13] for laser welded austenitic steels. The legend for both phase maps is given in Fig. 8b.

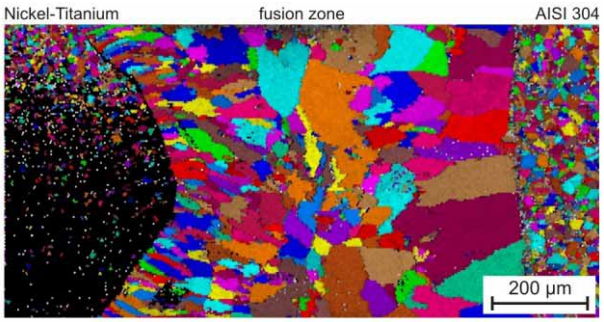

Fig 6: Map of the grain size and the grain distribution.

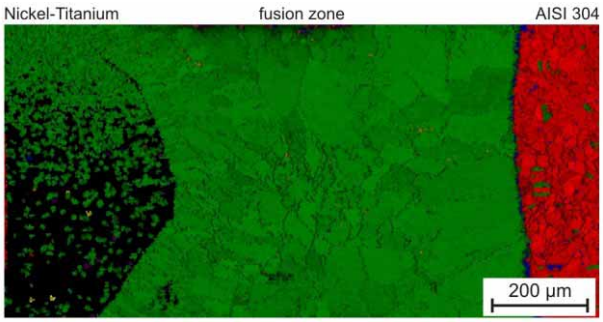

Fig 7: Map of the present phases in the dissimilar weld.

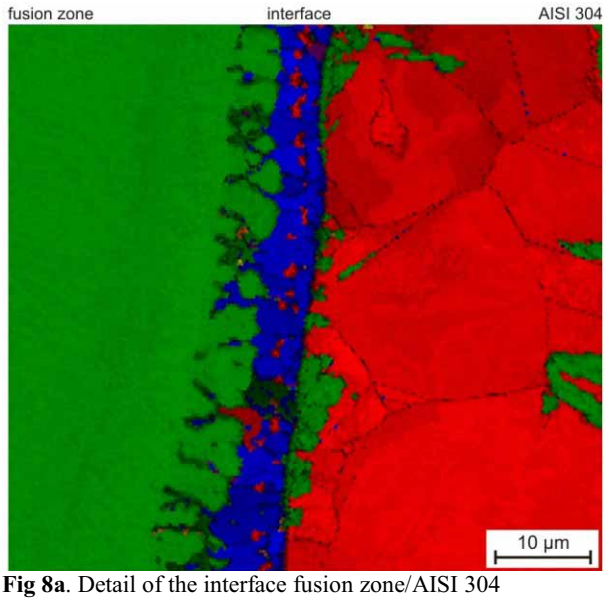

Fig 8a. Detail of the interface fusion zone/AISI 304

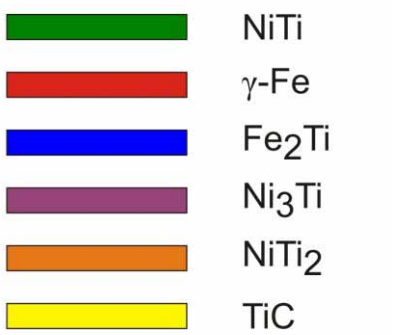

Fig.8b. Legend for the phase maps

3.4. Transmission electron microscopy (TEM)

TEM micrographs taken from specimen of the three different areas in the welding zone are presented in Fig. 9 where the extraction positions are marked in the upper left corner of the figures. The foil taken from the interface NiTi/fusion zone (Fig 9a) shows several larger grains. The main elements detected are Nickel and Titanium. The chemical composition in these grains is predominantly Ni-rich. Besides the Ni/Ti matrix there are two additional phases present. The first one is a dark, thin and longish phase located inside the grain. The Ni/Ti ratio of 1.5 which has been measured by EDX and TEM diffraction points to a precipitation of the TiC-Type. The second phases are round shaped dark colored particles mostly situated at the grain boundary (white arrow). The chemical composition of those showed high amounts of Ti, C and O (65 at.% Ti, 20at.% C and 15 at.% O). Due to that composition and due to the shape of the particles it could be concluded that it is a titanium oxycarbide

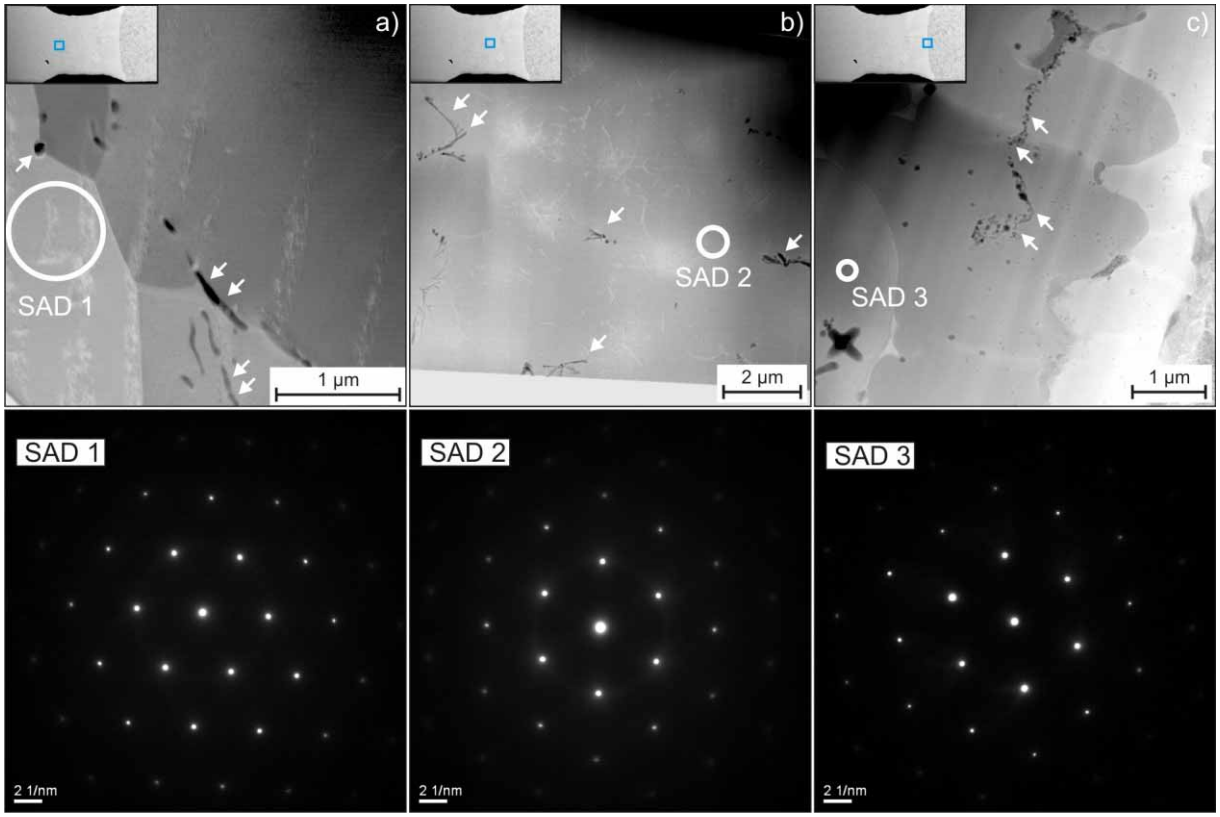

Fig. 9: TEM micrographs from foils of the interface NiTi/fusion zone a), fusion zone b) and interface fusion zone/AISI 304 c) with corresponding diffraction pattern. The extraction positions of the foils are marked in the micrograph in the upper left corner.

of the TiC_xO_y type as it has been described by Afir et al. [14]. The diffraction pattern (SAD 1) of the marked area shows a B2 structure. The micrograph in Fig. 9b of the specimen taken from the center of the fusion zone shows no grain boundaries due to the large grain size in that region. The average content of nickel is reduced down to 45 at.% Ni while the iron content is increased to more than 2 at.% Fe. Some dendritic shaped structures could be observed marked with the arrows in Fig 9b). This phase is consistent with the phases detected in the SEM micrographs (Fig.3a). The average composition of this fine dendritic shaped phase is 50 at.% Ti and 20 at.% C as well as 30 at.% Ni from the matrix. Therefore the phase could be identified as of the TiC type. The oyxcarbides are absent in this foil.

The specimen taken from the interface fusion zone/AISI304 does only show half of the complete interface zone at the steel side (fig. 9 c). In the uppermost left corner of the TEM-micrograph only the austenitic steel is present containing no titanium. The region with the brighter contrast shows a wavelike shape on the side facing the fusion zone. The Fe-content in this region is only 50 at.% while the Ni and Ti content are determined to approximately 16 at.% each. Fine particles containing Mn and Si from the AISI 304 base metal are distributed in the sample (white arrows). The fine bright line in the lower left part of the micrograph mainly consists of Ni and Ti bordering a region with a B2 containing up to 14 at.% Fe. Additionally the EDX measurements reveal a strong gradient for iron from 64 at.% Fe down to 14 at.% Fe in the direction to the fusion zone..

4. Summary and Conclusion

In this study the microstructure of laser welded NiTi/AISI 304 dissimilar joints was presented. The shift of the laser spot position provides a crack and pore free joint of the sheet materials. The phases were analyzed at the interfaces as well as in the fusion zone. According to the XRD, EBSD results and TEM diffraction a predominant B2 structure is present in the fusion zone. The interface on the AISI 304 side consists mainly of a Fe_2Ti-type intermetallic phase as verified by EBSD and local EDX measurements. In the fusion zone TiC-carbides and roundly shaped oxycarbides of TiC_xO_y-type could be observed. The mechanical properties of the joints and a more detailed study of the phases will be the topic of future works.

These studies were conducted under the SFB 459 research program and supported with funds from the “Deutsche Forschungsgemeinschaft”. We would like to thank Robert Zarnetta for kindly performing the XRD data. Special thank to Tobias Simon and Christoph Somsen for the support in the TEM investigations and André Oppenkowski for the assistance in evaluating the EBSD data.

5. References

[1] Y.T. Hsu, Y.R. Wang, S.K. Wu, C. Chen, Effect of CO_2 Laser Welding on the Shape-Memory and Corrosion Characteristics of TiNi Alloys Metallurgical and Materials Transactions A, Volume 32, Number 3, (2001) p. 569
[2] P. Schlossmacher, T. Haas and A. Schüssler: Laser-Welding of a Ni-Rich TiNi Shape Memory Alloy: Mechanical Behavior Journal de Physique IV, 7 (1997), C5/251-C5/256
[3] P. Schloßmacher, T. Haas, A. Schüßler: Laser welding of Ni-Ti shape memory alloys, Proc. SMST Pacific Grove, California USA (1994), pp. 85-90
[4] A. Falvo, F.M. Furgiuele, C. Maletta: Laser welding of a NiTi alloy: Mechanical and shape memory behaviour Materials Science and Engineering: A, 412, (2005), 235-240
[5] A. Tuissi, S. Besseghini, T. Ranucci, F. Squatrito, M. Pozzi Effect of Nd-YAG laser welding on the functional properties of the Ni–49.6at.%Ti Materials Science and Engineering A, 273-275, (1999), 813-817
[6] P.C. Hall, Laser welding Nitinol to Stainless Steel, Proc. SMST, Pacific Grove, California USA (2003), p. 219-228
[7] G. Wang: Welding of Nitinol to Stainless Steel, Proc. SMST Pacific Grove, California USA (1997), 131-136.
[8] H. Gugel, A. Schürmann, W. Theisen, Laser welding of NiTi wires, Materials Science and Engineering: A Volumes 481-482, (2008), p. 668-671
[9] H. Gugel, W. Theisen, Laserstrahlschweißen von Mikrodrähten aus Nickel-Titan-Formgedächtnislegierungen und austenitischem Stahl, Materialwissenschaft und Werkstofftechnik, Volume 38, Issue 6, (2007), p. 489
[10] K.H. Lo, C.H. Shek, J.K.L. Lai, Recent developments in stainless steels, Materials Science and Engineering R 65 (2009) p.39
[11] G.Cacciamani, R. Ferro, U.E. Klotz, J. Lacaze, P.Wollants, J. De Keyzer, Critical evaluation of the Fe-Ni, Fe-Ti and Fe-Ni-Ti alloy system, Intermetallics 14 (2006) p. 1312
[12] P. Riani, G. Cacciamani, J. Lacaze, Y. Thebaut, Phase equilibria and phase transformations in the Ti-rich corner of the Fe-Ni-Ti system, Intermetallics14 (2006) p. 1226
[13] H.K.D. Bhadeshia, S.A. David, J.M. Vitek, Solidification sequences in stainless steel dissimilar alloy welds, Materials Science and Technology, Vol. 7 (1991) p. 50-61
[14] A. Afir, M. Achour, N. Saoula, Journal of Alloys and Compounds 288 (1999) 124–140 X-ray diffraction study of Ti–O–C system at high temperature and in a continuous vacuum